Structural Engineering and Mechanics, Vol. 20, No. 5 (2005) 575-587
DOI: http://dx.doi.org/10.12989/sem.2005.20.5.575

Nonlinear analysis of interaction between flexible pile group and soil

Jie Liu†

College of Civil Engineering, Hunan University, Changsha, Hunan 410082, China
Department of Civil Engineering, Zhuzhou Institute of Technology, Zhuzhou, Hunan 412008, China

Q. S. Li‡

Department of Building and Construction, City University of Hong Kong, Hong Kong

Zhe Wu†

Department of Flight Vehicle Design and Applied Mechanics, Beijing University of Aeronautics and Astronautics, Beijing 100083, China

(Received June 14, 2004, Accepted April 25, 2005)

Abstract. Using the nonlinear load transfer function for pile side soil and the linear load transfer function for pile end soil, a combined approach of the incremental load transfer matrix method and the approximate differential equation solution method is presented for the nonlinear analysis of interaction between flexible pile group and soil. The proposed method provides an effective approach for the solution of the nonlinear interaction between flexible pile group under rigid platform and surrounding soil. To verify the accuracy of the proposed method, a static load test for a nine–pile group under a rigid platform is carried out. The finite element analysis is also conducted for comparison purposes. It is found that the results from the proposed method match very well with those from the experimental test and are better in comparison with the finite element method.

Key words: pile-soil interaction; settlement; load transfer; composite ground.

1. Introduction

Composite pile foundation, also known as small settlement pile foundation, is a kind of transition between natural and pile foundation. The most often seen flexible piles in composite foundations are: soil pile, ash-soil pile, lime pile, cement coal-ash granular pile, etc. As composite foundations are widely used in engineering practice, a question of how to determine

† Professor
‡ Associate Professor, Corresponding author, E-mail: bcqsli@cityu.edu.hk

the load carrying capacity and the settlement of the composite foundation become one of the most important problems in geotechnical engineering. In-situ static load test is considered as the most reliable method. However, the characteristics of composite foundations are that the pile and its surrounding soil both take load; therefore, relatively large area of loaded test is needed to get desired results. Large load test is relatively more expensive. Therefore, it is desirable to search for simple and satisfactory computational approaches that meet engineering accuracy. It is well known that, under foundation load, the loads carried by each flexible pile are different (Canetta and Nove 1989, Hooper 1973. Poulos and Davis 1980). How to determine the distribution of load for each pile and its surrounding soil under the foundation and the transfer rule for each pile are important research topics in the field of soft foundation engineering. Presently, the finite element method is the most commonly used method in the analysis of this type of composite foundation. In general, there are two types of finite element methods used in this field: the first one is the traditional "group pile" finite element method (Canetta and Nove 1989, Haddadin 1971, Balaam *et al.* 1977). This method requires separate elements for a pile and its surrounding soil in the reinforced area. Meanwhile, in order to simulate the pile-soil interaction between their boundaries, one can put a contact element at the interface. The advantage of this method is that it can analyze the loading mechanism of the soft foundation reinforced by flexible piles. However, for large-scale soft foundation reinforced by pile group, because of huge degrees of freedom involved, the calculation becomes very complicated and time consuming. The second method is the composite constitutional finite element method (Randolph and Worth 1978). This method regards the reinforced area as an inhomogeneous composite material made of piles and their surrounding soil, then the constitutional equations that govern the whole soft foundation reinforced by the flexible piles can be established. Finally, the finite element method is used to solve the equations. This method divides the foundation into discrete elements without consideration of the existence of the piles, therefore, the method can not take into account the interaction between the piles and their surrounding soil.

Juran and Riccobono (1991) concluded through experiment that the load transfer mechanism of a single pile is quite different under side load condition. They also stated that because the development of the load capacity of the soil between piles, the piles under composite foundations behave differently from a single free pile. Other researchers using Geddes stress coefficient studied the interaction between the pile box (mat) foundation and the surrounding soil according to the compatibility of the displacement of the pile and soil (Randolph and Worth 1979).

Because the load transfer method can reflect the nonlinear characteristics of the pile side soil relatively well (Liu *et al.* 2004), a case where nine piles under a stiff platform will be considered herein and the load transfer method will be used to analyze the nonlinear interaction between the piles and soil. For pile side soil, nonlinear load transfer function will be used. And for pile end soil, linear load transfer function will be adopted. This paper for the first time presents a combined approach of the incremental load transfer matrix method and the approximate differential equation solution method for the analysis of the title problem. To verify the accuracy of the proposed method, a static load test is carried out for a nine-pile group under a rigid platform. The finite element analysis is also conducted for comparison purposes. It is found that the results from the proposed method match very well with the data from the test and are in closer agreement with the measurements than those from the finite element method.

2. Pile side load transfer function and basic assumptions

2.1 Load transfer function

The skin friction (shear stress) at the shear surface between the pile and pile side soil can be described by the hyperbolic curve model as follows (Juran and Riccobono 1991, Xiao *et al.* 2002, 2003):

$$\tau(z) = \frac{w(z)}{a_0 + b_0 w(z)} \tag{1}$$

where $w(z)$ is the relative displacement at the shear surface, a_0 and b_0 are the parameters of the load transfer of the pile side soil.

Differentiating Eq. (1) can obtain the shear stiffness of the shear surface:

$$k(z) = \frac{a_0}{[a_0 + b_0 w(z)]^2} \tag{2}$$

2.2 Basic assumptions

To study the interaction between pile #1, 2 and 3, zones I, II and III are divided and shown in Fig. 1. From the load and geometric symmetry, it is observed that the shear stress on the boundary of zone I is equal to zero (Alamgir *et al.* 1996). Also, the shear stresses on boundary *BE*, *BC*, *FC*, *HC* for zones II and III are neglected. Considering the nonlinear behavior of the load transfer and the shear stiffness $k(z)$ change with z, each pile and the corresponding pile side soil are divided into N sections. In each section the local coordinate is established as z_{mi} ($i = 1, 2, \ldots, N$; $m = 1, 2, 3$),

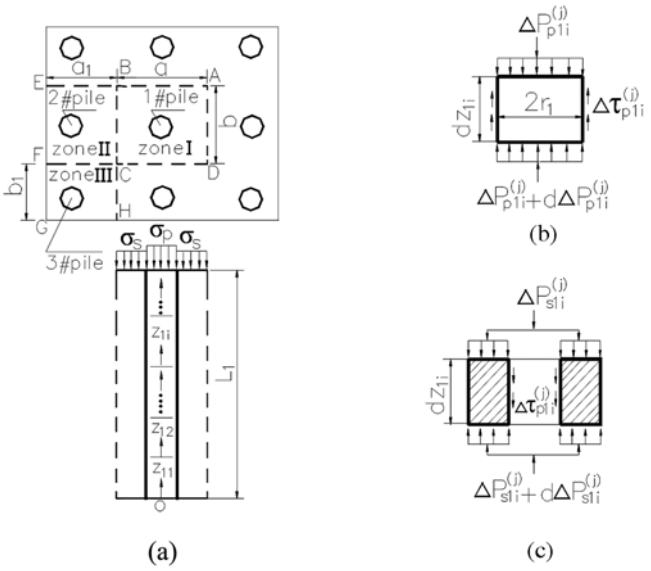

Fig. 1 (a) System of the pile-soil, (b)(c) Stresses acting on element of pile and soil, respectively

where m represents the number of pile. h_{mi} is the length of the i-th pile ($i = 1, 2, \ldots, N$). Also, the total load is the summation of the load increment acting on each subject, i.e., $P_{m0} = \Delta P_{m0}^{(1)} + \Delta P_{m0}^{(2)} + \ldots + \Delta P_{m0}^{(j)} + \ldots + \Delta P_{m0}^{(M_1)}$.

1) Neglecting the radial displacement of the pile side soil and the vertical displacement of soil outside the foundation; assuming the axial deformations of the pile and pile side soil are uniform.
2) Assuming the foundation is rigid, i.e., the vertical displacements at the bottom of the foundation are identical for each pile.
3) Assuming the relationships between the friction increment caused by various load increments for each section of the pile and its side soil and the relative displacement increment at the shear surface are linear, i.e.,

$$\Delta \tau_{pmi}^{(j)}(z_{mi}) = k_{pmi}[\Delta w_{pmi}^{(j)}(z_{mi}) - \Delta w_{smi}^{(j)}(z_{mi})] \tag{3}$$

$$\Delta \tau_{smi}^{(j)}(z_{mi}) = k_{smi}\Delta w_{smi}^{(j)}(z_{mi}) \tag{4}$$

where $\Delta \tau_{pmi}^{(j)}(z_{mi}), \Delta \tau_{smi}^{(j)}(z_{mi})$ are respectively the increments of friction on the i-th pile section and its surrounding soil induced by the j-th level load at the m-th pile. $\Delta w_{pmi}^{(j)}(z_{mi}), \Delta w_{smi}^{(j)}(z_{mi})$ are respectively the increments of axial displacement on the i-th pile section and its surrounding soil induced by the j-th level load at the m-th pile. k_{pmi} and k_{smi} are respectively the shear stiffness (kN/m^3) between the i-th pile and its surrounding soil, and the shear stiffness of the soil for the m-th pile under the j-th level of load. In the increment method of nonlinear analysis, usually they are substituted with the shear stiffness under the $(j-1)$th load increment; its value is obtained from the total relative displacement of both sides of the shear surface using Eq. (2). In this paper, the following two formulas are used to obtain k_{pmi} and k_{smi} under the j-th load increment.

For pile side:
$$k_{pmi} = \frac{a_0}{[a_0 + b_0(w_{pmi}^{(j-1)}(0) - w_{smi}^{(j-1)}(0))]^2} \tag{5}$$

Outside the boundary of the subject of the study:
$$k_{smi} = \frac{a_1}{[a_1 + b_1 w_{smi}^{(j-1)}(0)]^2} \tag{6}$$

where a_0, b_0, a_1 and b_1 are the parameters of the transfer function of the pile surrounding soil.

$$w_{pmi}^{(j-1)}(0) = \sum_{j=1}^{j-1} \Delta w_{pmi}^{(j)}(0)$$

$$w_{smi}^{(j-1)}(0) = \sum_{j=1}^{j-1} \Delta w_{smi}^{(j)}(0)$$

where $\Delta w_{pmi}^{(j)}(0)$ and $\Delta w_{smi}^{(j)}(0)$ are the axial displacement increments of the m-th pile induced by the j-th load increment at the bottom of the i-th section of the pile and its surrounding soil, respectively.

4) The resistance forces at the pile end and its surrounding soil are assumed to follow the linear models,

$$p_b = k_b s_b \tag{7a}$$

$$p_s = k_b s_s \tag{7b}$$

where k_b is the stiffness of compression of the soil at the pile end. s_b is the displacement at the pile end, and s_s is the displacement of the pile surrounding soil at the pile end.

3. Nonlinear analysis of the interaction between piles and soil

3.1 The interaction between number 1 pile and soil

The pile-soil system depicted in area I is selected as the study object. If the load increment $\Delta P_{10}^{(j)}$ is added to the object, then in the i-th segment of the pile at cross-section z_{1i} the increment of the internal force $\Delta P_{p1i}^{(j)}(z_{1i})$ will be induced. Considering the differential segment d_{z1i} of the i-th segment, as shown in Fig. 1(b), using the Hook's law and the equilibrium condition, the differential equation is:

$$\frac{d^2 \Delta w_{p1i}^{(j)}(z_{1i})}{dz_{1i}^2} = \frac{2k_{p1i}}{E_p r_1}[\Delta w_{p1i}^{(j)}(z_{1i}) - \Delta w_{s1i}^{(j)}(z_{1i})] \tag{8}$$

$$\Delta P_{p1i}^{(j)}(z_i) = -E_p \pi r_1^2 \frac{d\Delta w_{p1i}^{(j)}(z_{1i})}{dz_{1i}} \tag{9}$$

where E_p is the elastic modulus of the pile and r_1 is the radius of the pile.

The same analysis can be applied to the soil around the pile. The increment of the internal force $\Delta P_{s1i}^{(j)}(z_{1i})$ is induced by the increment load, the governing differential equation for the surrounding soil shown in Fig. 1(c) is,

$$\frac{d^2 \Delta w_{s1i}^{(j)}(z_{1i})}{dz_{1i}^2} = -\lambda_{s1i}^2[\Delta w_{p1i}^{(j)}(z_{1i}) - \Delta w_{s1i}^{(j)}(z_{1i})] \tag{10}$$

$$\Delta P_{s1i}^{(j)}(z_{1i}) = -E_s(ab - \pi r_1^2)\frac{d\Delta w_{s1i}^{(j)}(z_{1i})}{dz_{1i}} \tag{11}$$

where $\lambda_{s1i} = \sqrt{2\pi r_1 k_{p1i}/E_s(ab - \pi r_1^2)}$; E_s is the deformation modulus of the surrounding soil; the definitions of a and b are given in Fig. 1.

Combining Eqs. (8) and (10), one obtains

$$\frac{d^4 \Delta w_{p1i}^{(j)}(z_{1i})}{dz_{1i}^4} - \mu_i^2 \frac{d^2 \Delta w_{p1i}^{(j)}(z_{1i})}{dz_{1i}^2} = 0 \tag{12}$$

where $\mu_i = \sqrt{\lambda_{p1i}^2 + \lambda_{s1i}^2}$ $(i = 1, 2, \ldots, N)$; $\lambda_{p1i} = \sqrt{2k_{p1i}/E_p r_1}$.

Solving Eq. (12), we obtain,

$$\Delta w_{p1i}^{(j)}(z_{1i}) = c_1 + c_2 z_i + c_3 e^{\mu_i z_{1i}} + c_4 e^{-\mu_i z_{1i}} \quad (0 \le z_{1i} \le h_{1i}) \tag{13}$$

where $c_i (i = 1, 2, 3, 4)$ is undetermined coefficient.

Substituting Eq. (13) into Eq. (10), we have,

$$\Delta w_{s1i}^{(j)}(z_{1i}) = c_5 e^{\lambda_{s1i} z_{1i}} + c_6 e^{-\lambda_{s1i} z_{1i}} + c_1 + c_2 z_{1i} + A_i c_3 e^{\mu_i z_{1i}} + A_i c_4 e^{-\mu_i z_{1i}} \quad (0 \le z_{1i} \le h_{1i}) \tag{14}$$

where $A_i = -\lambda_{s1i}^2 / \lambda_{p1i}^2$ $(i = 1, 2, \ldots, N)$. $c_i (i = 5, 6)$ is undetermined coefficient.

From the differential equation theory it can be seen that Eq. (8) cannot be solved exactly by Eqs. (13) and (14). Therefore, an approximation method, the sub-domain method is used herein to solve Eq. (8). Eqs. (13) and (14) satisfy the following two integral equations, then they will satisfy Eq. (8) approximately.

$$\int_0^{\frac{h_{1i}}{2}} \left\{ \frac{d^2 \Delta w_{p1i}^{(j)}(z_{1i})}{dz_{1i}^2} - \frac{2k_{p1i}}{E_p r_1} [\Delta w_{p1i}^{(j)}(z_{1i}) - \Delta w_{s1i}^{(j)}(z_{1i})] \right\} dz_{1i} = 0 \tag{15}$$

$$\int_{\frac{h_{1i}}{2}}^{h_{1i}} \left\{ \frac{d^2 \Delta w_{p1i}^{(j)}(z_{1i})}{dz_{1i}^2} - \frac{2k_{p1i}}{E_p r_1} [\Delta w_{p1i}^{(j)}(z_{1i}) - \Delta w_{s1i}^{(j)}(z_{1i})] \right\} dz_{1i} = 0 \tag{16}$$

Substituting Eqs. (13) and (14) into Eqs. (15) and (16), we have,

$$c_5 = \eta_i c_3 + \xi_i c_4 \tag{17}$$

$$c_6 = \beta_i c_3 + \gamma_i c_4 \tag{18}$$

where $\eta_i = \alpha_i [1 - e^{(\mu_i + \lambda_{s1i}) h_{1i}/2}] / (1 - e^{\lambda_{e1i} h_{1i}})(e^{\lambda_{s1i} h_{1i}/2} - 1)$;

$\xi_i = \alpha_i e^{-\mu_i h_{1i}/2} [1 - e^{(\lambda_{s1i} - \mu_i) h_{1i}/2}] / (1 - e^{\lambda_{e1i} h_{1i}})(e^{\lambda_{s1i} h_{1i}/2} - 1)$;

$\beta_i = \alpha_i [1 - e^{(\mu_i - \lambda_{s1i}) h_{1i}/2}] / (e^{-\lambda_{s1i} h_{1i}} - 1)(e^{-\lambda_{s1i} h_{1i}/2} - 1)$;

$\gamma_i = \alpha_i e^{-\mu_i h_{1i}/2} [1 - e^{-(\mu_i + \lambda_{s1i}) h_{1i}/2}] / (e^{-\lambda_{s1i} h_i} - 1)(e^{-\lambda_{s1i} h_{1i}/2} - 1)$;

$\alpha_i = (1 - A_i - \mu_i^2 / \lambda_{p1i}^2)(e^{\mu_i h_{1i}/2} - 1) \lambda_{s1i} / \mu_i \quad (i = 1, 2, \ldots, N)$

Substituting Eqs. (13) and (14) into Eqs. (9) and (11), we obtain the increment of the axial forces $\Delta P_{p1i}^{(j)}(z_{1i})$ and $\Delta P_{s1i}^{(j)}(z_{1i})$.

3.2 Pile-soil interaction of number 2 and 3 piles

Using the same approach as that presented in section 3.1, we obtain the axial displacement increments of the pile number 2 and its surrounding soil.

$$\Delta w_{p2i}^{(j)}(z_{2i}) = c_{1e} e^{\mu_{1i} z_{2i}} + c_{2e} e^{-\mu_{1i} z_{2i}} + c_{3e} e^{\mu_{2i} z_{2i}} + c_{4e} e^{-\mu_{2i} z_{2i}} \ (0 \le z_{2i} \le h_{2i}) \tag{19}$$

$$\Delta w_{s2i}^{(j)}(z_{2i}) = c_{5e} e^{\lambda_{s2i} z_{2i}} + c_{6e} e^{-\lambda_{s2i} z_{2i}} + A_{1i} c_{1e} e^{\mu_{1i} z_{2i}} + A_{1i} c_{2e} e^{-\mu_{1i} z_{2i}} + A_{2i} c_{3e} e^{\mu_{2i} z_{2i}} + A_{2i} c_{4e} e^{-\mu_{2i} z_{2i}} \tag{20}$$

$$c_{5e} = \beta_{1i}c_{1e} + \gamma_{1i}c_{2e} + \beta_{2i}c_{3e} + \gamma_{2i}c_{4e} \tag{21}$$

$$c_{6e} = \eta_{1i}c_{1e} + \xi_{1i}c_{2e} + \eta_{2i}c_{3e} + \xi_{2i}c_{4e} \tag{22}$$

where $c_{ie}(i = 1, 2, 3, 4, 5, 6)$ is undetermined coefficient.

$$\mu_{1i} = \sqrt{(\lambda_{1i} + \sqrt{\lambda_{1i}^2 - 4\lambda_{2i}})/2}\ ;\ \mu_{2i} = \sqrt{(\lambda_{1i} - \sqrt{\lambda_{1i}^2 - 4\lambda_{2i}})/2}\ ;\ A_{ki} = \lambda_i^2/(\lambda_{s2i}^2 - \mu_{ki}^2)\ ;$$

$$\lambda_{1i} = (\lambda_{p2i}^2 + \lambda_{s2i}^2);\ \lambda_{2i} = \lambda_{p2i}^2(\lambda_{s2i}^2 - \lambda_i^2);\ \lambda_{p2i} = \sqrt{2k_{p2i}/E_p r_2}\ ;$$

$$\lambda_{s2i} = \sqrt{(bk_{s2i} + 2\pi r_2 k_{p2i})/E_s(a_1 b - \pi r_2^2)};\ \lambda_i = \sqrt{2\pi r_2 k_{p2i}/E_s(a_1 b - \pi r_2^2)}\ ;$$

$$\beta_{ki} = \alpha_{ki}(1 - e^{(\lambda_{s2i} + \mu_{ki})h_{2i}/2})/(1 - e^{\lambda_{s2i}h_{2i}})e^{\lambda_{s2i}h_{2i}/2}\ ;$$

$$\gamma_{ki} = \alpha_{ki}(e^{-\mu_{ki}h_{2i}/2} - e^{(\lambda_{s2i} - 2\mu_{ki})h_{2i}/2})/(1 - e^{\lambda_{s2i}h_{2i}})e^{\lambda_{s2i}h_{2i}/2}\ ;$$

$$\alpha_{ki} = \lambda_{s2i}e^{\lambda_{s2i}h_{2i}/2}(e^{\mu_{ki}h_{2i}/2} - 1)(1 - A_{ki} - \mu_{ki}^2/\lambda_{p2i}^2)/\mu_{ki}(e^{\lambda_{s2i}h_{2i}/2} - 1)\ ;$$

$$\eta_{ki} = \alpha_{ki} - \beta_{ki}e^{\lambda_{s2i}h_{2i}/2};\ \xi_{ki} = \alpha_{ki}e^{-\mu_{ki}h_{2i}/2} - \gamma_{ki}e^{\lambda_{s2i}h_{2i}/2}\ \ (k = 1, 2;\ i = 1, 2, \ldots, N)$$

Using the Hook's law and Eqs. (19) and (20), the increments of the axial force on the *i*-th segment and its surrounding soil of the number 2 pile, $\Delta P_{p2i}^{(j)}(z_{2i})$ and $\Delta P_{s2i}^{(j)}(z_{2i})$, can be found.

Substituting the subscript 2 with 3, the increments of the axial displacement $\Delta w_{p3i}^{(j)}(z_{3i})$, $\Delta w_{s3i}^{(j)}(z_{3i})$ and the increments of the axial force $\Delta P_{p3i}^{(j)}(z_{3i})$, $\Delta P_{s3i}^{(j)}(z_{3i})$ on the *i*-th segment of the number 3 pile and its surrounding soil can be found.

The axial displacement increments and force increments can be written in the following matrix form,

$$\begin{Bmatrix} \Delta X_{1i}^{(j)}(z_{1i}) \\ \Delta X_{2i}^{(j)}(z_{2i}) \\ \Delta X_{3i}^{(j)}(z_{3i}) \end{Bmatrix} = \begin{bmatrix} H_{1i}^{(j)}(z_{1i}) & 0 & 0 \\ 0 & H_{2i}^{(j)}(z_{2i}) & 0 \\ 0 & 0 & H_{3i}^{(j)}(z_{3i}) \end{bmatrix} \begin{Bmatrix} C_c \\ C_e \\ C_a \end{Bmatrix} \tag{23}$$

where $\Delta X_{1i}^{(j)}(z_{1i}), \Delta X_{2i}^{(j)}(z_{2i})$ and $\Delta X_{3i}^{(j)}(z_{3i})$ are respectively the state vector increments of piles 1, 2 and 3 and their surrounding soil under the *j*-th load increment. $\Delta X_{mi}^{(j)}(z_{mi}) = [\Delta w_{pmi}^{(j)}(z_{mi})\ \ \Delta P_{pmi}^{(j)}(z_{mi})\ \ \Delta w_{smi}^{(j)}(z_{mi})\ \ \Delta P_{smi}^{(j)}(z_{mi})]^T\ \ (m = 1, 2, 3)$; C_c, C_a, C_e are undetermined coefficient matrices, $C_c = [c_1\ \ c_2\ \ c_3\ \ c_4]^T$; $C_e = [c_{1e}\ \ c_{2e}\ \ c_{3e}\ \ c_{4e}]^T$; $C_a = [c_{1a}\ \ c_{2a}\ \ c_{3a}\ \ c_{4a}]^T$. $H_{mi}^{(j)}(z_{mi})$ is the transfer matrix.

$$H_{1i}^{(j)}(z_{1i}) = \begin{bmatrix} 1 & z_{1i} & e^{\mu_i z_{1i}} & e^{-\mu_i z_{1i}} \\ 0 & -E_p\pi r_1^2 & \varphi_i(z_{1i}) & \theta_i(z_{1i}) \\ 1 & z_{1i} & F_i(z_{1i}) & G_i(z_{1i}) \\ 0 & -E_s(ab - \pi r_1^2) & f_i(z_{1i}) & g_i(z_{1i}) \end{bmatrix}$$

$$H_{2i}^{(j)}(z_{2i}) = \begin{bmatrix} e^{\mu_{1i}z_{2i}} & e^{-\mu_{1i}z_{2i}} & e^{\mu_{2i}z_{2i}} & e^{-\mu_{2i}z_{2i}} \\ \varphi_{1i}(z_{2i}) & \theta_{1i}(z_{2i}) & \varphi_{2i}(z_{2i}) & \theta_{2i}(z_{2i}) \\ F_{1i}(z_{2i}) & G_{1i}(z_{2i}) & F_{2i}(z_{2i}) & G_{2i}(z_{2i}) \\ f_{1i}(z_{2i}) & g_{1i}(z_{2i}) & f_{2i}(z_{2i}) & g_{2i}(z_{2i}) \end{bmatrix}$$

Substituting the subscript 2 with 3 in $H_{2i}^{(j)}(z_{2i}), H_{3i}^{(j)}(z_{3i})$ is obtained.

where $\varphi_i(z_{1i}) = -E_p\pi r_1^2\mu_i e^{\mu_i z_{1i}};\ \theta_i(z_{1i}) = E_p\pi r_1^2\mu_i e^{-\mu_i z_{1i}};$

$$F_i(z_{1i}) = A_i e^{\mu_i z_{1i}} + \eta_i e^{\lambda_{s1i}z_{1i}} + \beta_i e^{-\lambda_{s1i}z_{1i}};$$

$$G_i(z_{1i}) = A_i e^{-\mu_i z_{1i}} + \xi_i e^{\lambda_{s1i}z_{1i}} + \gamma_i e^{-\lambda_{s1i}z_{1i}};$$

$$f_i(z_{1i}) = -E_s(ab - \pi r_1^2)(A_i\mu_i e^{\mu_i z_{1i}} + \eta_i\lambda_{s1i}e^{\lambda_{s1i}z_{1i}} - \beta_i\lambda_{s1i}e^{-\lambda_{s1i}z_{1i}});$$

$$g_i(z_{1i}) = -E_s(ab - \pi r_1^2)(-A_i\mu_i e^{-\mu_i z_{1i}} + \xi_i\lambda_{s1i}e^{\lambda_{s1i}z_{1i}} - \gamma_i\lambda_{s1i}e^{-\lambda_{s1i}z_{1i}});$$

$$\left.\begin{aligned} \varphi_{ki}(z_{2i}) &= -E_p\pi r_2^2\mu_{ki}e^{\mu_{ki}z_{2i}};\ \theta_{ki}(z_{2i}) = E_p\pi r_2^2\mu_{ki}e^{-\mu_{ki}z_{2i}} \\ F_{ki}(z_{2i}) &= \beta_{ki}e^{\lambda_{s2i}z_{2i}} + \eta_{ki}e^{-\lambda_{s2i}z_{2i}} + A_{ki}e^{\mu_{ki}z_{2i}} \\ G_{ki}(z_{2i}) &= \gamma_{ki}e^{\lambda_{s2i}z_{2i}} + \xi_{ki}e^{-\lambda_{s2i}z_{2i}} + A_{ki}e^{-\mu_{ki}z_{2i}} \\ f_{ki}(z_{2i}) &= -E_s(a_1b_1 - \pi r_2^2)(\beta_{ki}\lambda_{s2i}e^{\lambda_{s2i}z_{2i}} - \eta_{ki}\lambda_{s2i}e^{-\lambda_{s2i}z_{2i}} + A_{ki}\mu_{ki}e^{\mu_{ki}z_{2i}}) \\ g_{ki}(z_{2i}) &= -E_s(a_1b_1 - \pi r_2^2)(\gamma_{ki}\lambda_{s2i}e^{\lambda_{s2i}z_{2i}} - \xi_{ki}\lambda_{s2i}e^{-\lambda_{s2i}z_{2i}} - A_{ki}\mu_{ki}e^{-\mu_{ki}z_{2i}}) \end{aligned}\right\}(k = 1, 2)$$

The boundary conditions of the i-th segment and its surrounding soil are,

$$\left.\begin{aligned} \Delta w_{pmi}^{(j)}(z_{mi})\big|_{z_{mi}=0} &= \Delta w_{pmi}^{(j)}(0),\quad \Delta w_{smi}^{(j)}(z_{mi})\big|_{z_{mi}=0} = \Delta w_{smi}^{(j)}(0) \\ \Delta P_{pmi}^{(j)}(z_{mi})\big|_{z_{mi}=0} &= -\Delta P_{pmi}^{(j)}(0),\quad \Delta P_{smi}^{(j)}(z_{mi})\big|_{z_{mi}=0} = -\Delta P_{smi}^{(j)}(0) \end{aligned}\right\}(m = 1, 2, 3) \tag{24}$$

where $\Delta w_{pmi}^{(j)}(0)$ and $\Delta P_{pmi}^{(j)}(0)$ are respectively the displacement increment and the axial force increment of the m-th pile at the i-th segment under the j-th load increment. r_2 and r_3 are the radius of the piles 2 and 3, respectively. $\Delta w_{smi}^{(j)}(0)$ and $\Delta P_{smi}^{(j)}(0)$ are respectively the displacement increment and the axial force increment of the surrounding soils of the m-th pile at the i-th segment under the j-th load increment.

Substituting Eq. (24) into Eq. (23), we have,

$$\begin{Bmatrix} C_c \\ C_e \\ C_a \end{Bmatrix} = \begin{bmatrix} H_{1i}^{(j)}(0) & 0 & 0 \\ 0 & H_{2i}^{(j)}(0) & 0 \\ 0 & 0 & H_{3i}^{(j)}(0) \end{bmatrix}^{-1} \begin{Bmatrix} \Delta X_{1i}^{(j)}(0) \\ \Delta X_{2i}^{(j)}(0) \\ \Delta X_{3i}^{(j)}(0) \end{Bmatrix} \tag{25}$$

where $\Delta X_{mi}^{(j)}(0)(m = 1, 2, 3)$ are the state increment vector of the m-th pile at the i-th segment under the j-th load increment.

Substituting Eq. (25) into Eq. (23), we have,

$$\Delta X_i^{(j)}(z_{1i}, z_{2i}, z_{3i}) = D_i^{(j)}(z_{1i}, z_{2i}, z_{3i})\Delta X_i^{(j)}(0) \tag{26}$$

where $\Delta X_i^{(j)}(z_{1i}, z_{2i}, z_{3i}) = [\Delta X_{1i}^{(j)}(z_{1i}) \ \Delta X_{2i}^{(j)}(z_{2i}) \ \Delta X_{3i}^{(j)}(z_{3i})]^T$;

$\Delta X_i^{(j)}(0) = [\Delta X_{1i}^{(j)}(0) \ \Delta X_{2i}^{(j)}(0) \ \Delta X_{3i}^{(j)}(0)]^T$;

$$D_i^{(j)}(z_{1i}, z_{2i}, z_{3i}) = \begin{bmatrix} H_{1i}^{(j)}(z_{1i}) & 0 & 0 \\ 0 & H_{2i}^{(j)}(z_{2i}) & 0 \\ 0 & 0 & H_{3i}^{(j)}(z_{3i}) \end{bmatrix} \begin{bmatrix} H_{1i}^{(j)}(0) & 0 & 0 \\ 0 & H_{2i}^{(j)}(0) & 0 \\ 0 & 0 & H_{3i}^{(j)}(0) \end{bmatrix}^{-1}$$

The continuity condition for each segment is,

$$\Delta X_{i+1}^{(j)}(0) = \Delta X_i^{(j)}(h_{1i}, h_{2i}, h_{3i}) \quad (j = 1, 2, \ldots, M_1; \ i = 1, 2, \ldots, N-1) \tag{27}$$

where $\Delta X_{i+1}^{(j)}(0)$ is the state increment vector of the (i+1)-th segment under the j-th load increment at the bottom of the pile and its surrounding soil. $\Delta X_i^{(j)}(h_{1i}, h_{2i}, h_{3i})$ is the state increment vector of the i-th segment under the j-th load increment at the top of the pile and its surrounding soil.

$$\Delta X_{i+1}^{(j)}(0) = [\Delta X_{1i+1}^{(j)}(0) \ \Delta X_{2i+1}^{(j)}(0) \ \Delta X_{3i+1}^{(j)}(0)]^T$$

$$\Delta X_i^{(j)}(h_{1i}, h_{2i}, h_{3i}) = [\Delta X_{1i}^{(j)}(h_{1i}) \ \Delta X_{2i}^{(j)}(h_{2i}) \ \Delta X_{3i}^{(j)}(h_{3i})]^T$$

From Eqs. (26) and (27), we have,

$$\Delta X_N^{(j)} = \left(\prod_{i=N}^{1} D_i^{(j)}(h_{1i}, h_{2i}, h_{3i}) \right) \Delta X_b^{(j)} \tag{28}$$

where $\Delta X_N^{(j)} = [\Delta X_{1N}^{(j)}(h_{1N}) \ \Delta X_{2N}^{(j)}(h_{2N}) \ \Delta X_{3N}^{(j)}(h_{3N})]^T$;

$\Delta X_b^{(j)} = [\Delta X_{11}^{(j)}(0) \ \Delta X_{21}^{(j)}(0) \ \Delta X_{31}^{(j)}(0)]^T$;

$\Delta X_{mN}^{(j)}(h_{mN}) = [\Delta s_{pm}^{(j)} \ \Delta P_{pm}^{(j)} \ \Delta s_{tm}^{(j)} \ \Delta P_{tm}^{(j)}]^T$ (m=1, 2, 3);

$\Delta X_{m1}^{(j)}(0) = [\Delta s_{bm}^{(j)} \ -k_b A_{bm} \Delta s_{bm}^{(j)} \ \Delta s_{sm}^{(j)} \ -k_b A_{sm} \Delta s_{sm}^{(j)}]^T$ (m = 1, 2, 3)

$\Delta s_{pm}^{(j)}$ and $\Delta s_{tm}^{(j)}$ are respectively the settlement increments of the m-th pile under the i-th load increment. $\Delta P_{pm}^{(j)}$ and $\Delta P_{tm}^{(j)}$ are respectively the load increments at the top of the m-th pile under the j-th load increment. $\Delta s_{bm}^{(j)}$ and $\Delta s_{sm}^{(j)}$ are the displacement increments at the bottom of the m-th pile and its surrounding soil under the j-th load increment; A_{bm} and A_{sm} are the cross section areas of the m-th pile and the surrounding soil, respectively.

From Eqs. (26) and (27), the total displacement and internal force can be obtained as follows,

$$\left.\begin{aligned} w_{pmi}(z_{mi}) &= \sum_{j=1}^{j} \Delta w_{pmi}^{(j)}(z_{mi});\ w_{smi}(z_{mi}) = \sum_{j=1}^{j} \Delta w_{smi}^{(j)}(z_{mi}) \\ P_{pmi}(z_{mi}) &= \sum_{j=1}^{j} \Delta P_{pmi}^{(j)}(z_{mi});\ P_{smi}(z_{mi}) = \sum_{j=1}^{j} \Delta P_{smi}^{(j)}(z_{mi}) \end{aligned}\right\} \tag{29}$$

From Eq. (28), the load distributed to each pile and its surrounding soil P_{pm} and P_{tm} and the settlement at the top of the pile and its surrounding soil s_{pm} and s_{tm} under the j-th load can be obtained,

$$\left.\begin{aligned} s_{pm} &= \sum_{j=1}^{j} \Delta s_{pm}^{(j)};\quad s_{tm} = \sum_{j=1}^{j} \Delta s_{tm}^{(j)} \\ P_{pm} &= \sum_{j=1}^{j} \Delta P_{pm}^{(j)};\quad P_{tm} = \sum_{j=1}^{j} \Delta P_{tm}^{(j)} \end{aligned}\right\} \tag{30}$$

The proposed method can be used to determine the load-settlement curves for each pile and its surrounding soil under any platform load. Also it can be used to obtain the relationship between the cross-section axial force and the skin friction changing with depth.

4. Experimental and computational results

4.1 Experiment condition and content

Soil was uniformly distributed at the site for each case considered herein. Underground water depth was below 4.5 m. The soil was powder clay. Its physical coefficients were dry density $\gamma_d = 14.6$ kN/m^3, and liquidation limit $w_L = 30\%$, plastic index $I_p = 118.\%\%$, natural water content

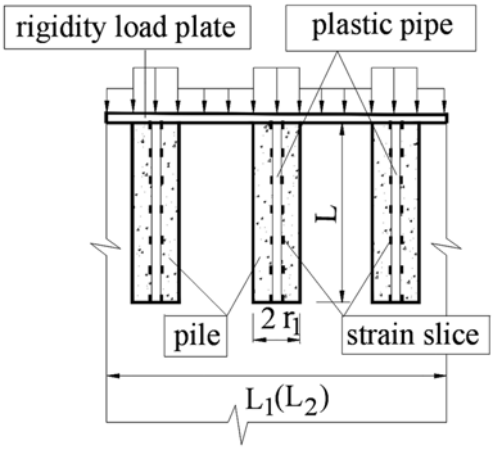

Fig. 2 Static load test of pile cap

$w = 20\%$, natural density $\gamma = 17.5$ kN/m^3. The on-site experiment conducted included rigid platform test (nine piles under the platform, as shown in Fig. 2) and foundation soil load test. A rectangular rigid plate $L_1 \times L_2 = 3.0 \times 3.0$ m was used for generating the loading. The flexible piles were a type of condensed cement-soil pile with 20% cement. From the experiment it was found that its 14 day compress strength with no lateral force $q_u = 4.6$ MPa, and Young's modulus $E_p = 365$ MPa. The manually dug and compacted pile was 3.50 m long with 0.35 m in diameter. The spacing between piles was 1.05 m. The center of the side pile to the edge of the platform was 0.45 m. At the axis of number 1, 2 and 3 piles, plastic pipes with diameter 3.0 cm were buried. The wall of the pipes was attached with strain gages. They located at 0.0 m, 0.5 m, 1.0 m, 1.5 m, 2.0 m, 2.5 m, 3.0 m and 3.5 m from the top of the piles (as shown in Fig. 2).

4.2 Results from the finite element analysis and the proposed method

In order to examine the accuracy of the proposed method, both experimental measurements and the finite element analysis were conducted to find the distribution of the pile friction along the length of the pile. When the finite element method was used, the calculation area was selected according to the previous studies (Schweigher and Pande 1986, Butterfield and Banerjee 1971). Also the load exerted on the loading plate was equivalent to the uniform load. The linear elastic or the Duncan hyperbolic curve model was used as the constitution model of the soil. The Young's modulus of the soil E_s was obtained from the soil load test and was found to be $E_s = 3.67$ MPa; the Poisson ratio was selected as 0.3. The Young's modulus of the plate was 2.06×10^5 MPa; the Poisson ratio of the pile and the plate was selected as 0.2. For Duncan hyperbolic curve model, the coefficients were $c = 16.0$ kPa and $\varphi = 24^\circ$. Other parameters included: elastic modulus number $K = 150$, unloading modulus number $K_{ur} = 368$, elastic modulus index $n = 0.35$, ratio of destruction $R_f = 0.85$, experiment constants of Duncan hyperbolic curve model were $G = 0.238$, $F = 0.15$ and $d = 3.16$. Using the proposed method, a pile and its surrounding soil were divided into 7 segments. The parameters of the transfer function of the pile surrounding soil were: $k_b = 1.35 \times 10^4$ kPa/m, $a_0 = 1.04 \times 10^{-4}$ m/kPa, $b_0 = 4.95 \times 10^{-2}$ kPa^{-1}, $a_1 = 1.174 \times 10^{-4}$ m/kPa, $b_1 = 5.0 \times 10^{-2}$ kPa^{-1}. Fig. 3 shows the results obtained from the proposed method and from the on-site test, when the load exerted on the pile cap was $P_0 = 880$ kN. It can be seen that: the most intense changes in the axial force occurred in the number 3 pile along the pile length, while the slowest changes occurred in the

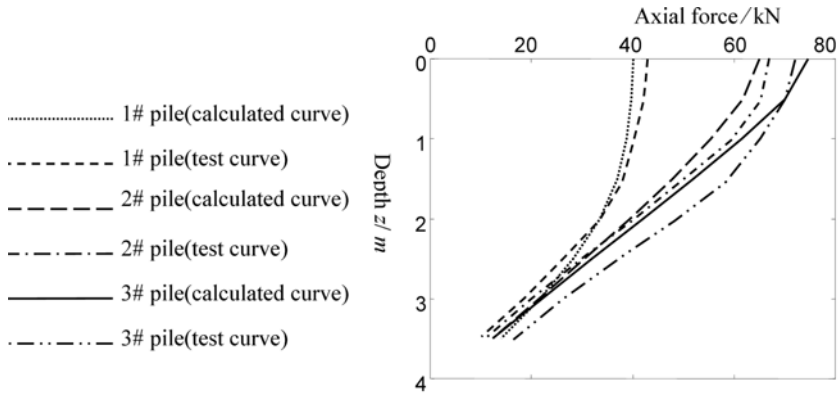

Fig. 3 Distribution of the axial force in pile section

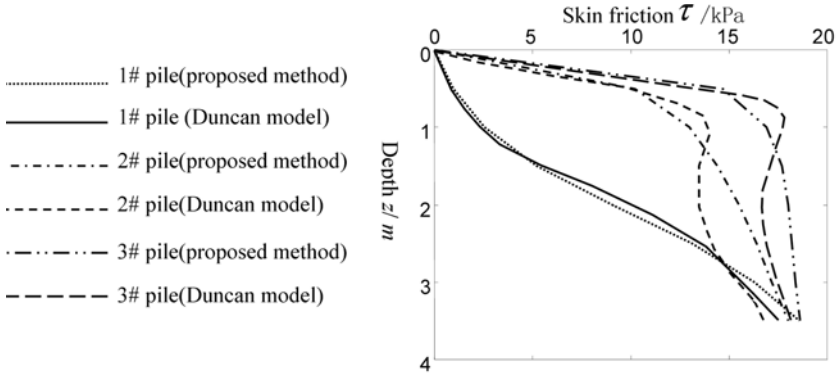

Fig. 4 Distribution of the skin friction along pile

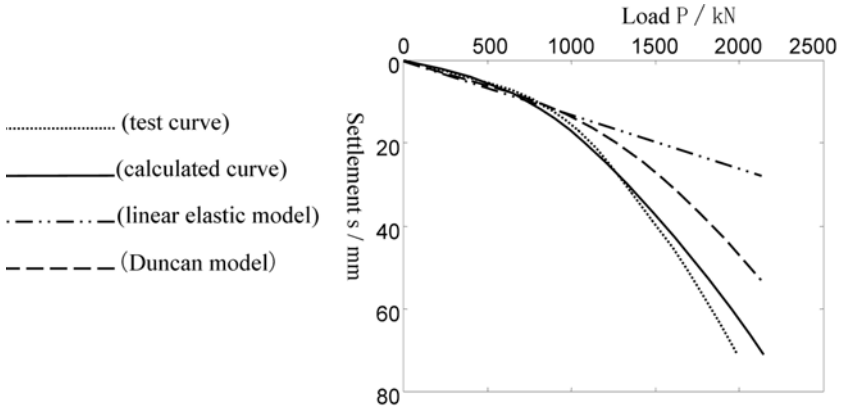

Fig. 5 Load-settlement curve of the piles cap

number 1 pile. This means that the pile friction is the largest for the number 3 pile and smallest for the number 1 pile. Also, it can be seen that the reaction on the top of the number 3 pile is the largest; the number 2 pile is the second; and the number 1 pile is the smallest. The ratios of these reactions are pile 1: pile 2: pile 3 = 1: 1.62: 1.88. Fig. 4 shows the results from the proposed method and Duncan hyperbolic curve model for $P_0 = 880$ kN. It can be seen that the pile friction is the largest for the number 3 pile, the number 2 pile is next and the number 1 pile is the smallest. Fig. 5 presents the results obtained by the proposed method is the closest to the experimental data, thus verifying the accuracy of the proposed mothod.

5. Conclusions

1. Using the nonlinear load transfer function for pile side soil and the linear load transfer function for pile end soil, a combined approach of the incremental load transfer matrix method and the approximate differential equation solution method was presented in this paper for nonlinear analysis of the interaction between flexible pile group and soil.
2. It was found that the distribution of pile friction was different for piles at different locations

under the rigid platform. The friction and the reaction in the corner of a pile is the largest, on the side is next and in the middle is the smallest.

3. The proposed method provides a new approach for the solution of the nonlinear interaction between flexible pile group and soil. The numerical example shows that the results determined from the proposed method match quite well with the experimental data and are in closer agreement with the measurements than those obtained from the finite element method, thus illustrating the proposed method is accurate and efficient.

Acknowledgements

The work described in this paper was fully supported by a grant from City University of Hong Kong (Project No. 7001591). We are thankful for the assistances provided by Dr. J. Tang in preparing the manuscript.

References

Alamgir, M., Miura, N., Poorooshasb, H.B. and Madhav, M.R. (1996), "Deformation analysis of soft ground reinforced by columnar inclusions", *Computers and Geotechnics*, **4**, 267-290.

Balaam, N.P., Poulos, H.G. and Brown, P.T. (1977), "Settlement analysis of soft clays reinforced with granular piles', *Proc. of the 5th Asian Regional Conf.*, Bangkok, **1**, 81-92.

Butterfield, R. and Banerjee, P.K. (1971), "The problem pile-group-pile cap interaction", *Geotechnique*, **21**, 282-297.

Canetta, G. and Nove, R. (1989), "A numerical method for the analysis of ground improved by columnar inclusions", *Computer and Geotechnics*, **7**, 99-114.

Haddadin, M.J. (1971), "Mats and combined footings analysis by the finite element methods", *Proc. ACI.*, **68**, 945-949.

Hooper, J.A. (1973), "Observation on the behaviour of a piled-raft foundation on London clay", *Proc. of the Institution of Civil Engineers,* **55**, 855-877.

Juran, I. and Riccobono, O. (1991), "Reinforced soft soil with artificially cemented compacted-sand columns", *J. of Geotechnical Engineering*, **117**, 1042-1060.

Liu, J., Xiao, H.B., Tang, J. and Li, Q.S. (2004), "Analysis of load-transfer of single pile in layered soils", *Computer and Geotechnics*, **31**, 127-135.

Poulos, H.G. and Davis, E.H. (1980), *Pile Foundation Analysis and Design*, New York: Wiley.

Randolph, M.F. and Worth, C.P. (1978), "Analysis of deformation of vertically loaded piles", *J. of the Geotechnical Engineering Division,* ASCE, **104**(12), 1465-1488.

Randolph, M.F. and Worth, C.P. (1979), "An analysis of vertical deformation of pile groups", *Geotechnique*, **29,** 423-439.

Schweiger, H.F. and Pande, G.N. (1986), "Numerical analysis of stone column supported foundations", *Computer and Geotechnics*. **2**, 347-372.

Xiao, H.B., Luo, Q.Z., Tang, J. and Li, Q.S. (2002), "Prediction of load-settlement relationship for large-diameter piles", *The Structural Design of Tall Buildings*, **11**(4), 295-308.

Xiao, H.B., Tang, J., Li, Q.S. and Luo, Q.Z. (2003), "Analysis of multi-braced earth retaining structures considering various excavation stages", *Proc. of The Institution of Civil Engineers, Structures and Buildings*, **156**(3), 307-318.